Cysteine Reactivity and Oligomeric Structures of Phospholamban and Its Mutants†

Christine B. Karim,‡ John D. Stamm,‡ Jawed Karim,‡ Larry R. Jones,*,§ and David D. Thomas*,‡

Department of Biochemistry, University of Minnesota Medical School, Minneapolis, Minnesota 55455, and Krannert Institute of Cardiology, Indiana University School of Medicine, Indianapolis, Indiana 46202

Received March 19, 1998; Revised Manuscript Received June 2, 1998

ABSTRACT: To test models for the pentameric structure of phospholamban (PLB) and study its structure and molecular dynamics in SDS solution, we characterized recombinant PLB and several of its mutants by (a) reactivity of cysteine residues toward DTNB [5,5′-dithiobis(2-nitrobenzoic acid)] and a thiol-reactive spin label, (b) oligomeric state on SDS−PAGE, and (c) EPR of the spin-labeled proteins. WT-PLB has three cysteine residues (36, 41, and 46), all located in the hydrophobic C-terminal transmembrane region. In SDS at pH 7.5, exhaustive reaction with either sulfhydryl reagent resulted in essentially 2 mol of cysteine reacted/mol of WT-PLB, with only slight destabilization of the native pentameric structure. When WT-PLB was denatured in guanidine at pH 8.1, all three cysteines reacted, disrupting the pentamer, which was restored upon cleavage of the disulfide bonds with DTT. In the tetrameric mutant C41L-PLB, the two remaining cysteine residues reacted, reversibly destabilizing the tetramer. In the monomeric mutant L37A-PLB, all three cysteines reacted. The pentameric double cysteine replacement mutant C36,46A-PLB showed negligible reactivity. We conclude that Cys-41 is the unreactive cysteine in PLB and is located at a crucial site for the maintenance of the pentameric structure. EPR spectra in SDS of spin-labeled WT-PLB and mutants correlate with the oligomeric state on SDS−PAGE; oligomeric proteins show decreased spin-label mobility compared with monomers. Molecular dynamics calculations were used to construct an atomic model for the transmembrane region of the PLB pentamer, constrained by previous mutagenesis results and the results of the present study. We conclude that (a) the mobilities of spin-labels attached to PLB and its mutants are sensitive to oligomeric state and (b) the pattern of cysteine reactivity, spin-label mobility, and oligomeric state supports a structural model for the PLB pentamer in which interactions between each pair of subunits are stabilized by a leucine−isoleucine zipper.

In cardiac SR,[1] the 52 amino acid integral membrane protein phospholamban (PLB) regulates the enzymatic activity of the Ca-ATPase (Ca pump) (*1*). PLB−ATPase interactions result in inhibition (*2*) and aggregation (*3*) of the Ca-ATPase. It has been established that the regulatory (inhibitory) effects of PLB on the cardiac Ca-ATPase are relieved by PLB phosphorylation at serine 16 (S) or threonine 17 (T), catalyzed by cAMP-dependent or Ca/calmodulin-dependent protein kinase, respectively (*4*).

Several different structural models have been proposed for PLB (*5*−*8*) and there is consensus on several key points. PLB is an amphipathic peptide with a hydrophilic N-terminus, which is predicted to be at least partially α-helical (*5*). The hydrophobic C-terminal amino acids (26−52) are known to form a transmembrane α-helical segment (*5*, *9*) and are involved in protein oligomerization (*10*). SDS−PAGE suggests that the quaternary structure of PLB is a homopentamer that is stabilized by the hydrophobic transmembrane domain (*10*).

Site-directed mutagenesis of PLB has identified several transmembrane residues that appear to be important for pentamer formation, as assayed by SDS−PAGE mobility (*11*−*14*). Mutation of amidated residues, to prevent hydrogen bonding, did not change the pentamer's thermal stability, while mutation of the three cysteines (residues 36, 41, and 46) to alanine or to serine decreased pentamer stability (*11*). The most striking effects of mutagenesis were produced by the mutation of certain leucines (residues 37, 44, and 51) or isoleucines (residues 40 or 47) to alanine; any one of these mutations produced profound destabilization of the pentamer on SDS−PAGE (*14*, *15*). For example, the mutant L37A-PLB migrated as a monomer on SDS−PAGE. Both WT-PLB and L37A-PLB bind to the Ca pump and inhibit Ca transport in the membrane, but the monomeric L37A-PLB has a stronger inhibitory effect than the pentameric WT-PLB (*16*). It has been suggested that the PLB monomer, not the pentamer, binds and inhibits the Ca pump in the SR membrane (*16*, *17*). This model is supported most

† This work was supported in part by grants to D.D.T. (GM27906) and the Minnesota Supercomputer Institute. L.R.J. was supported by grants (HL07308 and HL49428) from the National Institutes of Health. C.B.K. was supported by a Grant-In-Aid from the American Heart Association, Minnesota Affiliate.

* Address correspondence to D.D.T. or L.R.J.

‡ University of Minnesota Medical School.

§ Indiana University School of Medicine.

[1] Abbreviations: PLB, phospholamban; WT, wild type; SR, sarcoplasmic reticulum; OG, octyl glucoside; TAPS, *N*-[tris(hydroxymethyl)-methyl-3-aminopropanesulfonic acid; MOPS, 3-(*N*-morpholino)propanesulfonic acid; Tris, tris(hydroxymethyl)aminomethane; DTNB, 5,5′-dithiobis(2-nitrobenzoic acid); MTSSL, (1-oxy-2,2,5,5-tetramethyl-Δ^3-pyrroline-3-methyl)methanethiosulfonate; SDS, sodium dedecyl sulfate; PAGE, polyacrylamide gel electrophoresis; DTT, dithiothreitol; EPR, electron paramagnetic resonance; L37A, replacement of Leu-37 with alanine; C41L, replacement of Cys-41 with leucine; C36,46A, replacement of Cys-36 and Cys-46 with alanine.

S0006-2960(98)00642-4 CCC: $15.00
Published on Web 08/14/1998

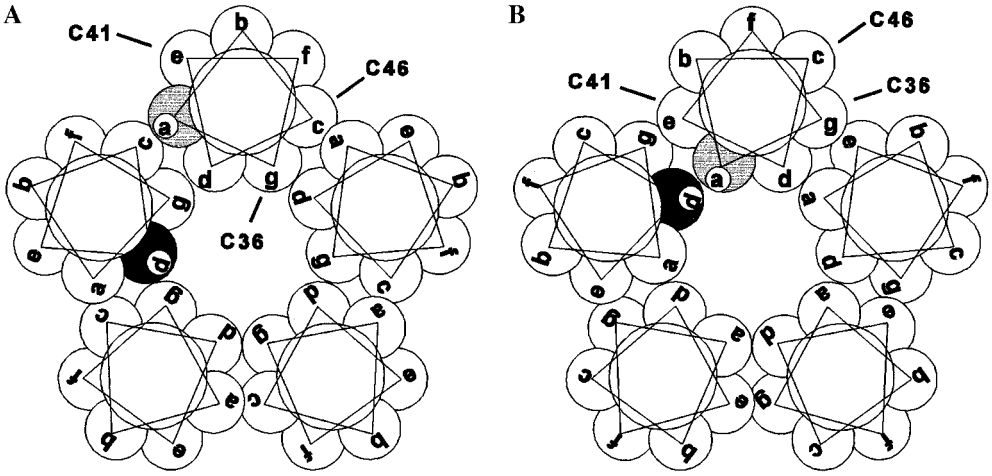

FIGURE 1: Helical wheel representation of the PLB transmembrane domain (residues 35−52). Panel A is based on the model of Engelman and co-workers (*19*), and panel B is adapted from Jones and co-workers (*15*). Both models are based on left-handed coiled coil structure, resulting in a 3.5 residue/turn repeat (heptad repeat). Equivalent positions occur every two turns and are identified by letters a−g. At this level of schematic representation, model B is related to model A by a counterclockwise rotation of each helix by one-seventh of a turn (one heptad position). The heptad positions containing the three cysteine residues are indicated, the position (a) containing the most critical leucine residues (37, 44, 51) is shown in gray, and the position (d) containing the most critical isoleucine residues (40, 47) is shown in black.

directly by measurements of oligomeric state in lipid bilayers, using boundary lipid EPR, which showed that WT-PLB and L37A-PLB both exhibit a dynamic equilibrium between monomers and oligomers that is shifted from monomer to oligomer by phosphorylation (*18*).

In the mutagenesis studies it was found that the key residues occurred every seven amino acids, forming a heptad repeat of mutational sensitivity. On the basis of these results, Simmerman et al. (*14*, *15*) proposed a schematic model (Figure 1B) for the PLB pentamer as a left-handed coiled coil stabilized specifically by interhelical interactions between leucines at one heptad position with isoleucines at another, i.e., a leucine−isoleucine "zipper". Therefore, it is important to understand the oligomeric structure of PLB in some detail.

Adams et al. (*19*) constructed an alternative model for the transmembrane domain of PLB, from a schematic representation of molecular dynamics simulations, with constraints based on the effects of random mutagenesis on SDS−PAGE of fusion proteins. This atomic model (Figure 1A) also proposes a left-handed coiled coil of five helices, but the contacts between the helices are quite different and do not support the proposal of the leucine−isoleucine zipper (Figure 1B).

A significant difference between these two models is highlighted when the positions of the three cysteine residues in the pentamer are examined. The model of Adams et al. (*19*) predicts that Cys-41 should be the most exposed of the three cysteines, while the model of Simmerman et al. (*15*) predicts that Cys-46 should be the most exposed (Figure 1).

Therefore, to assess the importance of the cysteine residues in phospholamban oligomer formation, and to distinguish between structural models of the PLB pentamer, we have reacted the cysteine residues of purified recombinant PLB and its mutants with thiol-reactive labels, including Ellman's reagent (DTNB) and a spin-label (MTSSL). Absorbance and EPR spectroscopy were used to study the pattern of cysteine reactivity, to determine the effects of cysteine modification on pentamer stability and to determine the mobility of the cysteine-bound spin-label. The results of these experiments were then used, in combination with molecular dynamics simulations, to test and refine molecular models for the PLB pentamer.

MATERIALS AND METHODS

Materials. Native PLB and its site-directed mutants (L37A-PLB, C41L-PLB, and C36,46A-PLB) were expressed in Sf21 insect cell culture and purified by monoclonal antibody affinity chromatography (*9*, *15*, *20*, *21*). The final concentrations of PLB and its mutants after purification were approximately 1 mg/mL in 0.9% OG, 88 mM MOPS, 18 mM glycine, and 5 mM DTT (pH 7.2). The amino acid sequences of PLB and mutants were confirmed by both cDNA and protein sequencing (*10*, *22*).

Polyacrylamide Gel Electrophoresis and Protein Assay. Protein concentration was determined by the method of Schaffner and Weissmann (*23*). SDS−PAGE of labeled and unlabeled peptide was performed using a 4% stacking gel and a 10−20% acrylamide gradient in the resolving gel, which was then stained with Coomassie Blue. Samples electrophoresed contained typically 2.5−4.0 μg of protein with 1% SDS in Tricine sample buffer (*24*).

Cysteine Modification of WT-PLB and Mutants with MTSSL. WT-PLB and its mutants in 88 mM MOPS, 0.9% OG, 18 mM glycine, and 5 mM DTT (pH 7.2) were concentrated and diluted 10 times continuously with 60 mM Tris and 0.1% SDS, pH 7.5, using a Centricon 3 filter (Amicon). The final concentration of WT-PLB and mutants was 0.7 mg/mL. One microliter of 0.1 M MTSSL in DMF was added to 50 μg of WT-PLB and mutants (71 μL of 0.7 mg/mL) in 60 mM Tris and 0.1% SDS, pH 7.5. The spin-labeling reaction was performed overnight at 4 °C. The methanethiosulfonate spin-label attaches with high specificity to sulfhydryl groups (*25*). The separation of the unreacted spin-label was carried out by size exclusion chromatography, using a HPLC Hydropore-5-SEC column (30 × 1.5 cm). The fractions were concentrated with speed vacuum, and the residue was resuspended in water to a final buffer concentration of 120 mM Tris and 0.2% SDS, pH 7.5 (2× SDS buffer).

EPR Spectroscopy. EPR spectra were acquired with an X-band Bruker ESP-300 spectrometer and a Bruker ER4201

cavity and digitized with the built-in microcomputer using Bruker OS-9-compatible ESP 1620 acquisition software. Conventional EPR spectra were obtained using 100 kHz field modulation, with a microwave field intensity of 0.14 G. Conventional EPR spectra were acquired using a 100 G sweep width. The samples were measured in glass capillaries. The sample concentration was around 0.1 mg of PLB/mL in the EPR experiments. Multiple scans were acquired and averaged as necessary in order to improve the signal-to-noise ratio. The sample temperature was controlled to within 0.1 °C with a nitrogen gas flow temperature controller and monitored with a Sensortek Bat-21 digital thermometer using an IT-21 thermocouple probe inserted into the top of the capillary, such that it did not interfere with spectral acquisition. All spectra were recorded at 25 °C. Spectra were obtained using 100 kHz field modulation with a peak-to-peak modulation amplitude of 2 G. Other instrument settings include a time constant of 40 ms and 40 s/scan.

Spectral Analysis. Conventional EPR spectra were downloaded to an IBM-compatible PC and analyzed with software developed in our laboratory by Roberta L. H. Bennett. The spin-label concentration was determined by calculation of the double integral and comparison to known spin-label standards. Spectral parameters such as hyperfine splittings ($2T_{\parallel}'$, outer splitting) were measured using this software. The apparent order parameter was then calculated from (*26*, *27*):

$$S \text{ (order parameter)} = \frac{T_{\parallel}' - T_0}{T_{\parallel}' - T_0}$$

where T_0 is the isotropic hyperfine splitting constant in the absence of anisotropic effects. $T_{\parallel}$ is the principal value of the hyperfine tensor for an axially symmetric system. One likely model for a spin-label's motion is "wobble in a cone" where the spin-label is constrained to move in a conical shaped region. This cone angle (θ_c) can be calculated from the apparent order parameter (S) from the expression:

$$S = {}^1/_2 \cos \theta_c(1 + \cos \theta_c)$$

Titration of Free Sulfhydryls with 5,5′-Dithiobis(2-nitrobenzoate) (DTNB; Ellman's Reagent). For the determination of the total sulfhydryl group content, WT-PLB and its mutants were dissolved in 60 mM Tris and 0.1% SDS, pH 7.5 (SDS buffer), or in 6 M guanidine hydrochloride, 200 mM TAPS, and 2% Triton X-100, pH 8.1 (GHCl buffer). DTNB solution was added (from 10 mM in DMF) to the cell (final concentration 0.3 mM), and the absorbance at 410 nm was recorded versus time. After development of the maximum color (a consequence of the spontaneous hydrolysis of DTNB) the absorbance was extrapolated to zero time. The protein solution was added to the cell (final concentration: 6 μM in SDS buffer, 3 μM in GHCl buffer), and the determination of the modified sulfhydryl group was measured from the release of 2-nitro-5-mercaptobenzoic acid at 410 nm (*28*).

Phospholamban Modeling. The atomic model of phospholamban by Engelman and co-workers (*19*) was obtained from the Protein Data Bank (*29*) (PDB entry 1psl). Each individual helix was then rotated around its long axis by about one-seventh turn (ca. 51.4°), to an orientation consistent with the leucine−isoleucine zipper model of Jones and co-workers (*15*), so that Leu-37, Leu-44, Leu-51 and Ile-40 Ile-47 occupied the a and d positions, respectively (Figure 1B) (*15*). The model was then subjected to 2500 energy minimization steps, using the conjugate gradient method. Modeling made use of the Biosym/MSI software package InsightII/Discover, version (95.0), using consistent valence force field parameters (cvff).

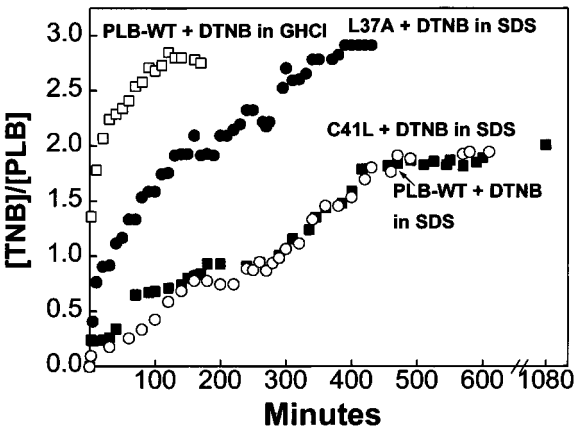

FIGURE 2: Cysteine reactivity (moles of TNB reacted per 6 kDa protomer) of WT-PLB (■), C41L-PLB (○), and L37A-PLB (●) in SDS buffer and WT-PLB (□) in GHCl buffer.

RESULTS

Cysteine Reactivity of WT-PLB and Two Mutants. The reactivity of WT-PLB and two of its mutants, L37A-PLB and C41L-PLB, with DTNB in SDS solution is shown in Figure 2. For WT-PLB approximately 2 mol (1.99 ± 0.01) of DTNB reacted/mol of PLB, suggesting that two of the three cysteine residues (36, 41, and 46) are reactive. When WT-PLB was denatured in GHCl, all three (3.06 ± 0.31) cysteines rapidly reacted. In the mutant C41L-PLB (Cys-41 to Leu), which is tetrameric on SDS−PAGE (*15*), both (2.08 ± 0.13) cysteine residues reacted with DTNB, while in the monomeric mutant L37A-PLB (Leu-37 to Ala) (*15*), all three cysteines (2.96 ± 0.04) reacted. Essentially the same results were found with a thiol-reactive spin-label (MTSSL). WT-PLB and its mutants were reacted with MTSSL, under conditions similar to those used above for DTNB, and incorporation of the spin-label was then quantified. For WT-PLB and C41L-PLB, only 2 mol (1.98 ± 0.02 and 1.95 ± 0.03) of MTSSL reacted/mol of PLB, while with L37A-PLB all three (3.18 ± 0.12) cysteines reacted with the spin-label.

SDS−PAGE. The oligomeric state of the unlabeled and labeled proteins was determined by SDS−PAGE. WT-PLB is predominantly pentameric both before (Figure 3A, lane 2) and after (Figure 3A, lane 3) reaction with DTNB. Smaller oligomers and monomers are also evident after labeling, indicating slight destabilization of the pentamer. After reaction of all three cysteines in guanidine at pH 8.1 (Figure 2), the pentamer remained completely disrupted even after guanidine was removed, resulting primarily in monomers and dimers on the gel (Figure 3A, lane 4). This effect was reversible, since the pentamer was restored by unblocking the disulfide bond with DTT (Figure 3A, lane 5). In the mutant C41L-PLB, which is mostly tetrameric on SDS−PAGE before labeling (Figure 3B, lane 3), both of the remaining cysteines reacted with DTNB (Figure 2), com-

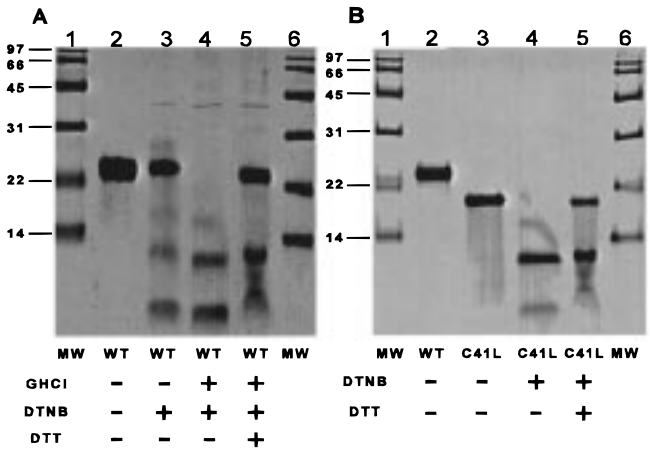

FIGURE 3: SDS−PAGE of (a) WT-PLB and (b) C41L-PLB. Lanes 1 and 6 in (A) and (B) contain the molecular weight standards (MW) with corresponding masses (kDa) on the left. DTNB (+) or (−) signifies whether the protein has been exhaustively labeled with DTNB (Figure 2). Labeling was done in either the presence (+) or absence (−) of GHCl. The samples were loaded in either the presence (+) or absence (−) of 10% DTT.

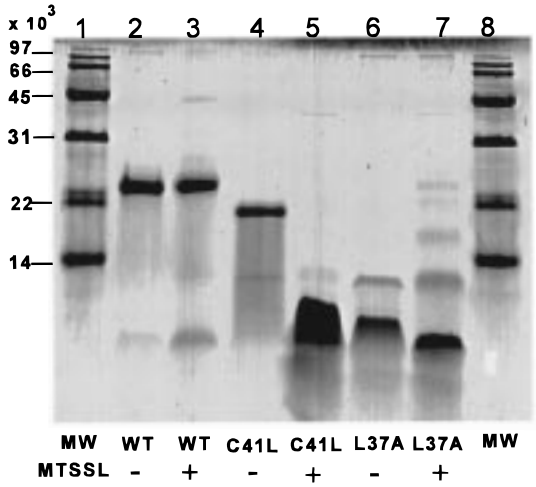

FIGURE 4: SDS−PAGE of MTSSL-labeled (+) and unlabeled (−) WT-PLB, C41L-PLB, and L37A-PLB. Lanes 1 and 8 are molecular weight standards (MW).

pletely disrupting the tetramer and resulting in dimers and monomers (Figure 3B, lane 4). The tetramer was partially recovered by the addition of DTT (Figure 3B, lane 5). The mutant L37A-PLB showed no change in its monomeric form on SDS−PAGE after complete labeling of its three cysteines (not shown).

The effects of exhaustive MTSSL labeling (Figure 4) on the SDS−PAGE oligomeric state were very similar to the effects of DTNB (Figure 3). WT-PLB is predominantly pentameric before (Figure 4, lane 2) and after (Figure 4, lane 3) reaction with 2 equiv of MTSSL. Both remaining cysteines of C41L-PLB reacted with MTSSL, with disruption of the oligomeric structure (Figure 4, lanes 4 and 5). All three cysteines of L37A-PLB reacted with MTSSL, with no change in the mostly monomeric structure (Figure 4, lanes 6 and 7).

EPR Spectra of Exhaustively Spin-Labeled WT-PLB and Mutants in SDS. Figure 5 represents EPR studies of the rotational dynamics of PLB exhaustively spin-labeled in SDS. The EPR spectra of the two spin-labeled mutants, C41L-PLB and L37A-PLB, which are both monomers in

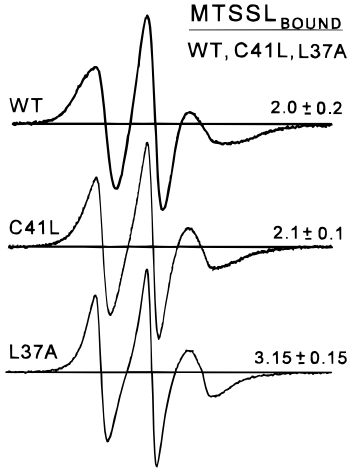

FIGURE 5: EPR spectra of fully MTSSL-labeled WT-PLB, C41L-PLB, and L37A-PLB. Spin-labeled peptides (1.6 mM) were in 120 mM Tris and 0.2% SDS, pH 7.5. Spectra were obtained at 25 °C and normalized to the double integral. The stoichiometries of MTSSL/mol of peptide were obtained through EPR spectral analysis and are listed on the right side of each spectrum (see also Table 1).

SDS after complete labeling (Figure 4), show single spectral components with high rotational mobility (Figure 5, middle and bottom), while the spectrum of the pentameric WT-PLB (Figure 5, top) indicates much more restriction of the spin-label motion. This restriction of probe motion is probably due to the oligomeric structure.

Reactivity of a PLB Mutant Containing Only One Cysteine. Since both WT-PLB and C41L-PLB contribute two reactive sulfhydryls, the results suggest that Cys-41 is the unreactive cysteine residue in WT-PLB. However, this conclusion is ambiguous, since the labeling of C41L disrupts the oligomeric structure. We attempted to use protein sequencing to determine which cysteines in WT-PLB were labeled by DTNB and MTSSL, but this was not feasible due to technical difficulties. Therefore, we analyzed the double cysteine mutant C36,46A in which cysteine residues 36 and 46 were changed to Ala, leaving residue 41 as the only cysteine. This mutant retains the predominantly pentameric structure of WT-PLB (Figure 6, lane 2). The extent of reaction of C36,-46A was 0.12 ± 0.02 mol with DTNB and 0.15 mol with MTSSL, indicating that Cys-41 is much less reactive than the other two cysteine residues in WT-PLB. The partial disruption of the pentameric structure (Figure 6, lane 3) suggests that a spin-label attached to Cys-41 cannot be accommodated in the pentamer.

Figure 7 summarizes the determination of cysteine reactivity for PLB and its mutants. The data for DTNB and MTSSL are in good agreement, showing that approximately 2 mol of cysteine are reactive in WT-PLB and C41L-PLB, 3 mol in the monomeric L37A-PLB, and none in C36,46A-PLB. Therefore, in the PLB pentamer, the only unreactive cysteine is Cys-41.

DISCUSSION

Cysteine Modification of WT-PLB and Mutants. To determine which cysteines are reactive and how this affects current structural models of the PLB pentamer (*15*, *19*), we have investigated the cysteine reactivity of WT-PLB and its mutants to DTNB and MTSSL. DTNB and MTSSL react

Table 1: Cysteine Modification of WT-PLB and Mutations with DTNB and MTSSL[a]

peptide	bound TNB/peptide	bound SL/peptide	predominant species on SDS−PAGE	$2T_{\parallel}'$ (G)	cone angle (deg)	order parameter
WT-PLB	1.99 ± 0.01 (n = 2)	1.98 ± 0.02 (n = 4)	pentamer	39.8 ± 1.3 (n = 2)	53.7 ± 2.2	0.24 ± 0.03
WT-PLB + GHCl	3.06 ± 0.31 (n = 2)		monomer	N/A	N/A	N/A
C41L	2.08 ± 0.13 (n = 2)	1.95 ± 0.03 (n = 4)	monomer	37.3 ± 0.2 (n = 3)	58.7 ± 0.4	0.17 ± 0.01
L37A	2.96 ± 0.04 (n = 2)	3.18 ± 0.12 (n = 2)	monomer	37.2 ± 0.1 (n = 2)	58.8 ± 0.1	0.17 ± 0.01
C36,46A	0.10 (n = 1)	0.15 (n = 1)	pentamer	N/A	N/A	N/A

[a] Each value represents the mean and SD for the number of measurements indicated in parentheses. N/A indicates that the experiment was not performed (EPR of WT-PLB + GHCl) or that the EPR spectrum had insufficient intensity to justify quantitative line-shape analysis (EPR of C36,46A)

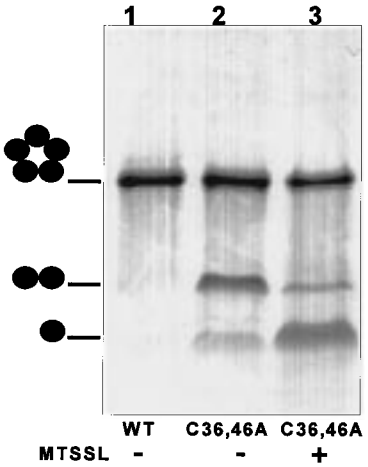

FIGURE 6: SDS−PAGE of unlabeled and labeled C36,46A-PLB. The peptides were electrophoresed under the same conditions as the SDS−PAGE in Figure 3. Lanes 1 and 2 are unlabeled WT-PLB and C36,46A-PLB in 1% SDS and Tris/Tricine buffer. Lane 3 presents C36,46A-PLB after being labeled at 0.15 MTSSL/peptide.

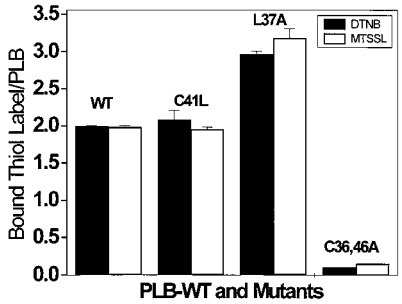

FIGURE 7: Direct comparison of the labeling stoichiometries between DTNB and MTSSL for WT-PLB, C41L-PLB, L37A-PLB, and C36,46A-PLB.

by the same mechanism, forming a stable disulfide bond between the cysteine sulfhydryl group and the labeling molecules. Cysteine reactivities and EPR spectra were measured in SDS to facilitate direct comparison with the oligomeric state determined by SDS−PAGE. Table 1 summarizes the results.

Exhaustive reaction of WT-PLB in SDS resulted in only approximately 2 mol of cysteine reacted/mol of PLB (Table 1), regardless of reagent, with no significant effect on SDS−PAGE pentamer stability. Upon denaturation of WT-PLB in GHCl, all three cysteines (Table 1) were reactive with either reagent, and the pentameric form was not evident on SDS−PAGE, even after the removal of the GHCl (Figure 3A, lane 4). When DTT was added, unblocking the cysteines, the pentameric form was restored (Figure 3A, lane 5). These results suggest that one of the three cysteine residues of WT-PLB is located at the interface between subunits in the PLB pentamer, at a position that would cause this residue to have low accessibility and where the pentameric structure cannot sterically accommodate a significant addition of mass.

All three cysteines of L37A-PLB, which is monomeric on SDS−PAGE (Figure 4, lane 6), completely reacted with DTNB or MTSSL (Table 1). C41L-PLB displayed the same extent of reaction to both DTNB and MTSSL (Table 1) as WT-PLB, but the unlabeled form migrates as a tetramer on SDS−PAGE (Figure 3B, lane 3), while labeling disrupts that form into monomers (Figure 3B, lane 4). Thus, the reaction of the two remaining cysteines, after the mutation of Cys-41 to Leu, disrupts the oligomeric structure, as does the labeling of all three cysteines in WT-PLB. Therefore, only in the monomeric form, obtained through either mutation (L37A-PLB) or denaturation (GHCl), are all three cysteines reactive, and perturbation of all three cysteines (labeled WT-PLB in GHCl or labeled C41L-PLB) destabilizes the oligomer.

To further elucidate which of the three cysteines is unreactive, we studied the mutant C36,46A-PLB, which contains only a single cysteine at position 41. This mutant is predominantly pentameric on SDS−PAGE (Figure 6) and has very low reactivity to both DTNB and MTSSL (Table 1). These results show clearly that *Cys-41 is the unreactive cysteine* in the PLB pentamer, suggesting that the pentameric structure occludes the Cys-41 sulfhydryl. The labeling of Cys-41 disrupted the pentameric structure of both WT-PLB (Figure 3, lane 4) and the single Cys mutant C36,46A (Figure 6, lane 3), indicating that *Cys-41 is in a position in the pentameric structure that does not tolerate addition of mass*. This conclusion is consistent with the observation that substitution of Cys-41 with a bulky phenylalanine produces PLB monomers, whereas substitution of the other two cysteines with phenylalanine does not (*15*). Simmerman et al. (*15*) have suggested that the side chain at position 41 is instrumental in governing the number of subunits in the oligomer, since PLB packs as a tetramer when cysteine is replaced with the bulkier side chain of leucine (C41L).

Spin-Label Mobility Is Sensitive to Oligomeric States of PLB and Mutants. The EPR results (Figure 5) support conclusions based on SDS−PAGE. Compared to WT-PLB (two cysteines labeled, Table 1), the spectra of L37A-PLB (all three cysteines labeled, Table 1) and C41L-PLB (both cysteines labeled, Table 1) display narrower line widths and splittings, indicating greater spin-label mobility. This correlates well with the differences in oligomeric state on SDS−PAGE. Labeled L37A-PLB and C41L-PLB, which are both

primarily monomeric (Figure 4, lanes 7 and 5, respectively), show greater spin-label mobility than WT-PLB, which is mainly pentameric. This strongly suggests that in WT-PLB protein−protein interactions between subunits cause the spin-label motions to be restricted, broadening the EPR lines. This restriction in the spin-label motion could be due to three factors at a molecular level: an increase in the size of the rotating oligomer that decreases the rate of overall rotational motion, an increase in the rigidity of the peptide backbone, or an increase in the specific steric packing around the spin-labeled side chain (*30*). Although it is unclear exactly which molecular interactions are the cause of these differences in spin-label mobility, this detection of protein oligomerization is a novel application of the site-directed spin-labeling method.

Since L37A-PLB has one site (Cys-41) labeled that is not labeled in WT-PLB, the difference between their EPR spectra could arise because of either the different labeling sites or the different oligomeric structure. However, in C41L-PLB, the same sites are labeled as in WT-PLB, so the differences in EPR spectra between these two labeled proteins probably directly reflect the differences in their oligomeric states.

The order parameters calculated from the EPR spectra (Table 1) indicate the degree of restriction experienced by the spin-label. WT-PLB, which is predominantly pentameric on SDS−PAGE, has a higher order parameter, indicating greater spin-label restriction, than that observed for L37A-PLB and C41L-PLB, which are chiefly monomeric on SDS−PAGE. An effective cone angle, describing the angular amplitude of dynamic disorder experienced by the spin-label, can be calculated from the EPR order parameters (Table 1). Although other models for restricted rotation might be applicable, this cone angle is a useful estimate of the amplitude of the spin-label's motion. A smaller cone angle, indicating more restricted motion, is found for the primarily pentameric WT-PLB than for the primarily monomeric species, L37A-PLB and labeled C41L-PLB. This strong correlation between oligomerization and spin-label restriction should be applicable for future EPR experiments involving both lipid and the Ca-ATPase.

Specific Role of Cys-41 in the Transmembrane Region of WT-PLB and Mutants. The roles of the transmembrane cysteine residues have been investigated through site-directed mutagenesis (*11*, *13*, *15*). MacLennan and co-workers (*11*) suggested that the cysteine residues are essential for the high degree of stability of the oligomeric structure, probably due to the size and polarity of the cysteine residues matching the hydrophobic microenvironment formed by the surrounding amino acids. It has been shown that the PLB quaternary structure is intolerant of changes in Cys-41, since pentamer formation was disrupted by changing Cys-41 to either Leu, Phe (*15*), or Ser (*11*). Therefore, Simmerman et al. (*15*) proposed that Cys-41 is confined to an interfacial cleft between adjacent helices and suggested that specific contacts of residues 37−41 are primarily responsible for stabilizing the pentameric PLB assembly. In contrast, in the model of Adams et al. (*19*), Cys-41 is exposed to the exterior of the pentamer, Cys-46 is packed in the helix interface, and Cys-36 is aligned toward the interior of the pentamer (*31*).

The present study has shown that Cys-41 has very low reactivity when PLB is pentameric, becoming reactive only when the protein is unfolded (6 M GHCl) or monomeric (L37A-PLB). The pentameric structure appears to occlude the sulfhydryl side chain of Cys-41 in such a way as to make it unreactive. Covalent labeling of WT-PLB at Cys-41, which is only possible in the presence of GHCl, prevents the reassembly of the pentameric structure. This is probably due to the addition of the mass of the label, disrupting the hydrophobic packing involved in the interface between helices, as has been demonstrated for the C41F mutation (*11*, *15*). Thus our results seem more consistent with the arrangement of subunits predicted by Simmerman et al. (*15*) (Figure 1B) than those predicted by the atomic model of Adams et al. (*19*). Therefore, we carried out molecular dynamics simulations in order to obtain an atomic model of the PLB transmembrane domain that is consistent with the subunit packing predicted by Simmerman et al. (*15*).

Molecular Dynamics Simulations. We started our modeling with the coordinates of the model of Adams et al. (*19*) that were obtained by molecular dynamics and simulated annealing, using a global search to find reasonable structures for the PLB pentamer. Adams et al. used these calculations to produce a handful of energetically favorable structures and then selected one of these, based on the effects of mutagenesis on SDS−PAGE mobility of a fusion protein of staphylococcal nuclease and PLB mutants. In the resulting pentamer model (Figure 8A), adjacent PLB protomers interact at helical positions d and g (Figure 8A, top).

We manipulated this structure until the key leucines were near the key isoleucines, as required for the leucine−isoleucine zipper proposed by Simmerman et al. (*15*). Specifically, we rotated each individual helix counterclockwise along its long axis to allow heptad positions a (containing leucines 37, 44, and 51) and d (containing isoleucines 40 and 47) to line up and then performed a molecular dynamics simulation to obtain an energy-minimized structure (Figure 8B). This model was found to be energetically similar to the model of Adams et al. (*19*) after both were energy minimized, but the refined model (Figure 8B) has several features that make it more plausible.

The new atomic model (Figure 8B) shows that the Leu−Ile zipper is clearly a realistic structure. Even after energy minimization, the Leu-37, Leu-44, and Leu-51 side chains (red) interdigitate with the side chains of Ile-40 and Ile-47 (blue) from the adjacent helix in the new model (B), while the model of Adams et al. (A) clearly lacks these interactions. In addition, an interesting implication arises from this new model when the exposure of the cysteine sulfhydryl groups are examined (shown in yellow). The original model of Adams et al. (*19*) (Figure 8A) places Cys-41 in a position in the pentamer that would apparently be exposed to solvent, while Cys-36 and Cys-46 would be occluded. In contrast, the pattern of sulfhydryl accessibility that arises from a leucine−isoleucine zipper model (Figure 8B) agrees with our reactivity results. The Cys-46 sulfhydryl is visible only from the pentamer exterior (OUT), while the Cys-41 sulfhydryl is visible only from the interior (IN), and Cys-36 is partially exposed to both surfaces. The inequivalent exposures of Cys-36 and Cys-41 were not obvious from the schematic helix-packing model (Figure 8B, top), although Simmerman et al. proposed, on the basis of mutagenesis data, that Cys-41 was more occluded. The structural detail provided by the atomic model of Figure 8B explains how the Leu−Ile zipper results in the observed inequivalence of reactivity and

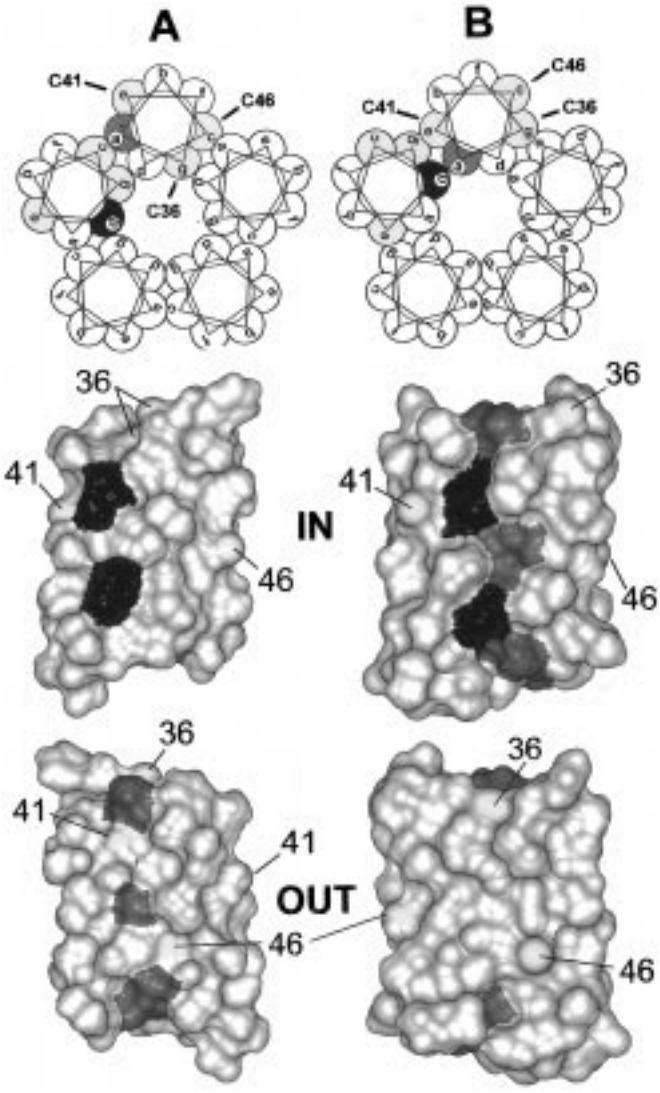

FIGURE 8: Two models for the pentameric structure of the PLB transmembrane domain (residues 35−52). Column A: Based on the model of Engelman and co-workers (*19*). Column B: Based on the proposal of Jones and co-workers (*15*). Top row: Helical wheel representation, as shown in Figure 1. Each PLB transmembrane helix is represented by a helical wheel with seven points (heptad repeat) indicative of a left-handed coiled coil. Points a and d on the helical wheel represent the interdigitating Leu and Ile residues that form the proposed Leu/Ile zipper. Point e is shaded and contains Cys-41. The other cysteine locations are indicated at points c and g. Bottom two rows: Computer-simulated atomic models, in Connolly surface representation, showing two of the helices in the pentamer. The left side (A) is a model proposed by Adams et al. (*19*), obtained from the Brookhaven Protein Data Bank (1psl) (*29*). The right side (B) shows our new model (see Materials and Methods). Leu-37, Leu-44, and Leu-51 of one monomer are highlighted in red, while Ile-40, and Ile-47 of the adjacent monomer are colored blue. Also, the sulfur atoms of the cysteine residues are colored yellow (six, in each model). Two views are shown: from the inside of the oligomer (IN) and the outside (OUT).

structural importance of the cysteines. *Thus, while the molecular modeling calculations do not produce a unique structural model for the PLB pentamer, the refined model we propose is energetically similar to the previously proposed model (19) and agrees more completely with the mutagenesis results (11−15) and our cysteine reactivity experiments*.

Conclusions. We conclude that Cys-41 is the least reactive cysteine in WT-PLB and is at a position in the pentameric structure that is crucial for maintenance of the oligomer. These results are consistent with a refined atomic model for the pentameric structure of PLB, integral to which is the critical role of a leucine−isoleucine zipper in maintaining pentameric stability (Figure 8B). The results further establish EPR as a technique that is sensitive to oligomeric interactions within PLB. The sulfhydryl group of Cys-41 at position e in the heptad model (Figure 8B) is probably involved in a specific interaction with residues at position d. This agrees with the proposal by Simmerman et al. (*15*) that specific contacts in the region of residues 37−41 are primarily responsible for maintaining oligomeric stability, as well as defining the number of protomers composing the multimer. The techniques used in the present study are sensitive to the oligomeric state of PLB and its mutants in SDS, as shown by the direct correlation with SDS−PAGE results. This study establishes the feasibility for application of these techniques, especially EPR, to studies of PLB oligomeric structure in lipid and in the presence of the Ca-ATPase. Furthermore, this study demonstrates the importance of experimental evidence beyond mutagenesis results in constraining a computer-simulated molecular model of a membrane protein.

ACKNOWLEDGMENT

We thank Germana Paterlini and Robert Milius for assistance with computer modeling and the Minnesota Supercomputer Institute for providing computational facilities. We also thank J. M. Autry for helpful comments on the manuscript.

REFERENCES

1. Lindemann, J., Jones, L., Hathaway, D., Henry, B., and Watanabe, A. (1983) *J. Biol. Chem. 258*, 464−471.
2. Tada, M., and Katz, A. M. (1982) *Annu. Rev. Physiol. 44*, 401−423.
3. Voss, J., Jones, L. R., and Thomas, D. D. (1994) *Biophys. J. 67*, 190−196.
4. Wegener, A. D., Simmerman, H. K. B., Lindemann J. P., and Jones, L. R. (1989) *J. Biol. Chem. 264*, 11468−11474.
5. Simmerman, H. K. B., Lovelace, D. E., and Jones, L. R. (1989) *Biochim. Biophys. Acta 997*, 322−329.
6. Young, E. F., McKee, M. J., Ferguson, D. G., and Kranias, E. G. (1989) *Membr. Biochem. 8*, 95−106.
7. Toyofuku, T., Kurzydlowski, K., Tada, M., and MacLennan, D. H. (1994) *J. Biol. Chem. 269*, 3088−3094.
8. Tada, M. (1992) *Ann. N.Y. Acad. Sci. 671*, 92−103.
9. Tatulian, S. A., Jones, L. R., Reddy, L. G., Stokes, D. L., and Tamm, L. K. (1995) *Biochemistry 34*, 4448−4456.
10. Simmerman, H. K. B., Collins, J. H., Theibert, J. L., Wegener, A. D., and Jones, L. R. (1986) *J. Biol. Chem. 261*, 13333−13341.
11. Fujii, J., Maruyama, K., Tada, M., and MacLennan, D. H. (1989) *J. Biol. Chem. 264*, 12950−12955.
12. Toyofuku, T., Kurzydlowski, K., Lytton, J., and MacLennan, D. H. (1992) *J. Biol. Chem. 267*, 14490−14496.
13. Arkin, I. T., Adams, P. D., MacKenzie, K. R., Lemmon, M. A., Brunger, A. T., and Engelman, D. M. (1994) *EMBO J. 13*, 4757−4764.
14. Simmerman, H. K. B., Kobayashi, Y. M., Strifler, B., and Jones, L. R. (1994) *Biophys. J. 66*, A 178.
15. Simmerman, H. K. B., Kobayashi, Y. M., Autry, J. M., and Jones, L. R. (1996) *J. Biol. Chem. 271*, 5941−5946.

16. Autry, J. M., and Jones, L. R. (1997) *J. Biol. Chem. 272*, 15872−15880.
17. Kimura, Y., Kurzydlowski, M., Tada, M., and MacLennan, D. H. (1997) *J. Biol. Chem. 272*, 15061−15064.
18. Cornea, R. L., Jones, L. R., Autry, J. M., and Thomas, D. D. (1997) *Biochemistry 36*, 2960−2967.
19. Adams, P. D., Arkin, I. T., Engelman, D. M., and Brünger, A. T. (1995) *Nat. Struct. Biol. 2*, 154−162.
20. Reddy, L. G., Jones, L. R., Cala, S. E., O'Brain, J. J., Tatulian, S. A., and Stokes, D. L. (1995) *J. Biol. Chem. 270*, 9390−9397.
21. Reddy, L. G., Jones, L. R., Pace, R. C., and Stokes, D. L. (1996) *J. Biol. Chem. 271*, 14964−14970.
22. Fujii, J., Uneo, A., Kitano, K., Tanaka, S., Kadoma, M., and Tada, M. (1987) *J. Clin. Invest. 79*, 301−304.
23. Schaffner, W., and Weissman, C. (1973) *Anal. Biochem. 56*, 502−514.
24. Schagger, H., and Jagow, G. (1987) *Anal. Biochem. 166*, 368−379.
25. Berliner, L. J., Grunwald, J., Hankovsky, H. O., and Hideg, K. (1982) *Anal. Biochem. 119*, 450.
26. Gaffney, B. J. (1976) in *Spin Labeling, Theory and Applications* (Berliner, L. J., Ed.) pp 567−571, Academic Press, Inc., New York.
27. Squier, T. C., and Thomas, D. D. (1989) *Biophys. J. 56*, 735−748.
28. Habeeb, A. F. S. A. (1972) *Methods Enzymol. 25*, 457.
29. Bernstein, F. C., Koetzle, T. F., Williams, G. J. B., Meyer, E. F., Jr., Brice, M. D., Rodgers, J. R., Kennard, O., Shimanouchi, T., and Tasumi, M. (1977) *J. Mol. Biol. 112*, 535−542.
30. Mchaourab, H. S., Lietzow, M. A., Hideg, K., and Hubbell, W. L. (1996) *Biochemistry 35*, 7692−7704.
31. Arkin, I. T., Adams, P. D., Brünger, A. T., Aimoto, S., Engelman, D. M., and Smith, S. O. (1997) *J. Membr. Biol. 155*, 199−206.

BI980642N